Supplementary information

Cavities in Context: Distinct Positional Consequences of Cavities on the Folding Landscape of a Repeat Protein

Kelly A. Jenkins[1], Martin J. Fossat[2#], Siwen Zhang[3], Durgesh K. Rai[4], Sean Klein[5], Richard Gillilan[4], Zackary White[6], Grayson Gerlich[6], Scott A. McCallum[7], Roland Winter[8], Sol Gruner[9], Doug Barrick[5] and Catherine A. Royer[1,2,3*]

www.pnas.org/cgi/doi/10.1073/pnas.1807379115

Table S1. Thermodynamic parameters from unfolding of the L83A and L109A variants of pp32							
Variant/ Perturbation	**Parameter**	**NMR**				**Fluorescence**	**Circular Dichroism[2]**
		Methyl Peak ~0.92 ppm	**Methyl Peak ~0.85 ppm**	**Backbone –NH**	**Trp155 indole NH <F and U>**		
L83A Pressure*	**ΔG (kcal/mol)**	-4.5 ± 0.2	-4.2 ± 0.1	-4.5 ± 0.4	-4.3 ± 0.3	-3.8 ± 0.2	
	ΔV (ml/mol)	169 ± 6	159 ± 5	168 ± 12	158 ± 11	135 ± 7	
L83A Urea	**ΔG (kcal/mol)**						4.46 ± .02
	m-value kcal/(mol*M urea)						3.25 ± .02
L109A Pressure	**ΔG (kcal/mol)**	-4.3 ± 0.9	-3.2 ± 0.8	-4.4 ± 0.7	-4.4 ± 0.3	-3.8 ± 0.2	
	ΔV (ml/mol)	192 ± 35	145 ± 27	183 ± 31	177 ± 11	159 ± 3	
L109A Urea	**ΔG (kcal/mol)**						4.56 ± .08
	m-value kcal/(mol*M urea)						3.37 ± .17

Table S2. Parameters from fits of C-terminal residue amide NH cross peak intensities of the L60A pp32 variant to a three-state unfolding model

Residue	ΔG_{NI} (kcal/mol)	ΔV_{NI} (ml/mol)	ΔG_{IU} (kcal/mol)	ΔV_{IU} (ml/mol)
104	-1.49	132	0.26	15
113	-2.63	163	-0.90	33
114	-2.04	127	-0.29	15
117	-1.76	105	-1.01	33
141	-2.00	125	-0.65	23
142	-2.04	128	-0.62	13
144	-2.84	135	-1.14	46
145	-1.98	125	-0.40	15
148	-1.51	97	-0.92	31
Average ± S.D.	-2.03 ± .43	126 ± 18	-.63 ± .41	24 ± 11

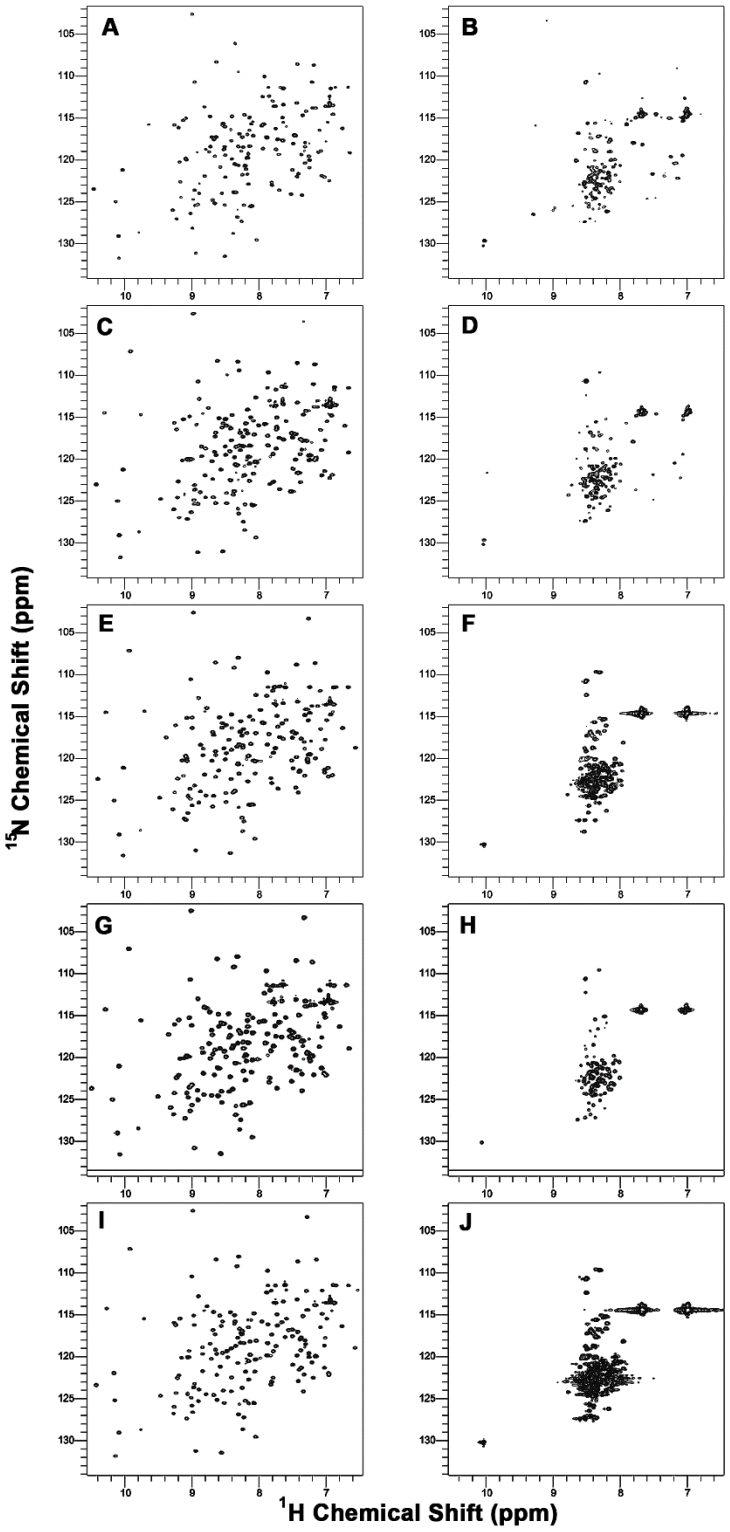

Figure S1. ^{15}N-^{1}H HSQC spectra for the pp32 cavity containing variants at atmospheric pressure (left column) and 2500 bar (right column). (A and B) I7A, (C and D) L60A, (E and F) L83A, (G and H) L109A and (I and J) L139A.

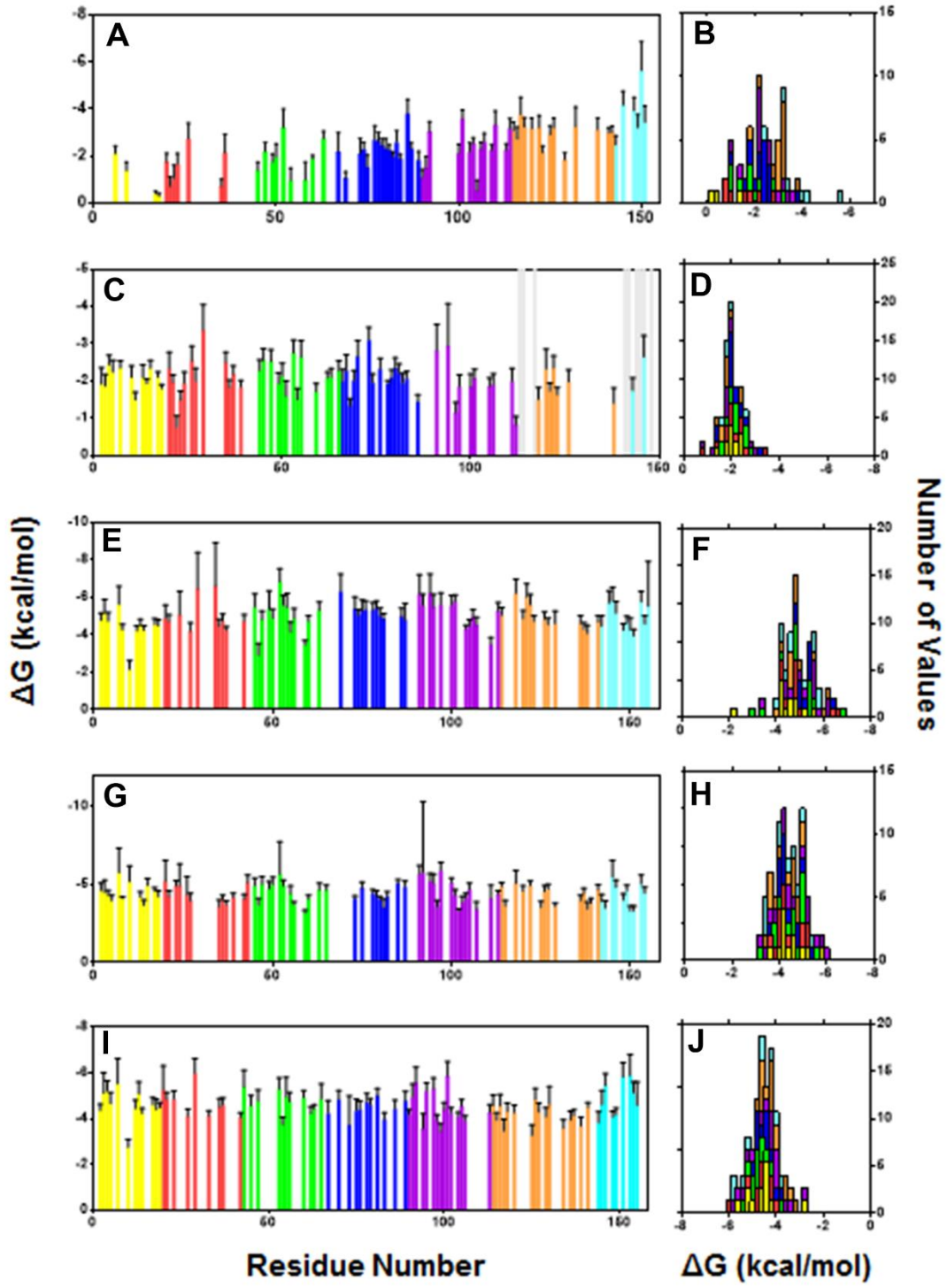

Figure S2. Free energy changes determined from the residue-specific pressure-induced unfolding transitions monitored by ^{15}N-^{1}H HSQC for the cavity containing variants of pp32. (A and B) I 7A, (C and D) L60A, E and F) L83A, G and H) L109A and I and J) L139A. Individual peak transitions were fit to a two-state unfolding model as described in the main text. Error bars represent the off-diagonal elements of the covariance matrix. Bars are colored per repeat as in Figure 1.

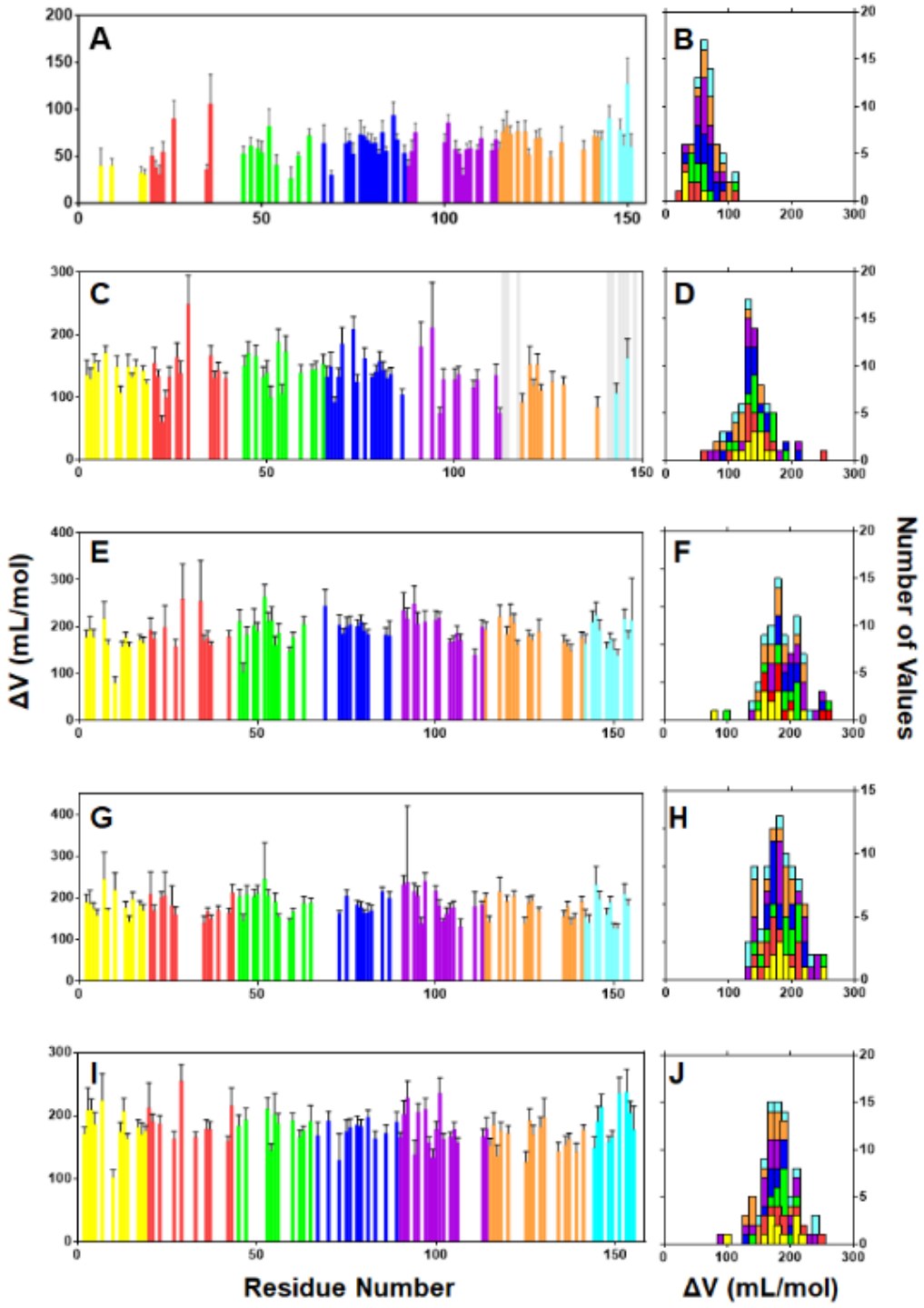

Figure S3. Volume change of the residue-specific pressure-induced unfolding transitions monitored by ^{15}N-^{1}H HSQC for the pp32 cavity containing variants. (A and B) I 7A, (C and D) L60A, (E and F) L83A, (G and H) L109A and (I and J) L139A. Individual peak transitions were fit to a two-state unfolding model as described in the main text. Bars for individual residues are colored per repeat as in Figure 1. Error bars represent the off-diagonal elements of the covariance matrix

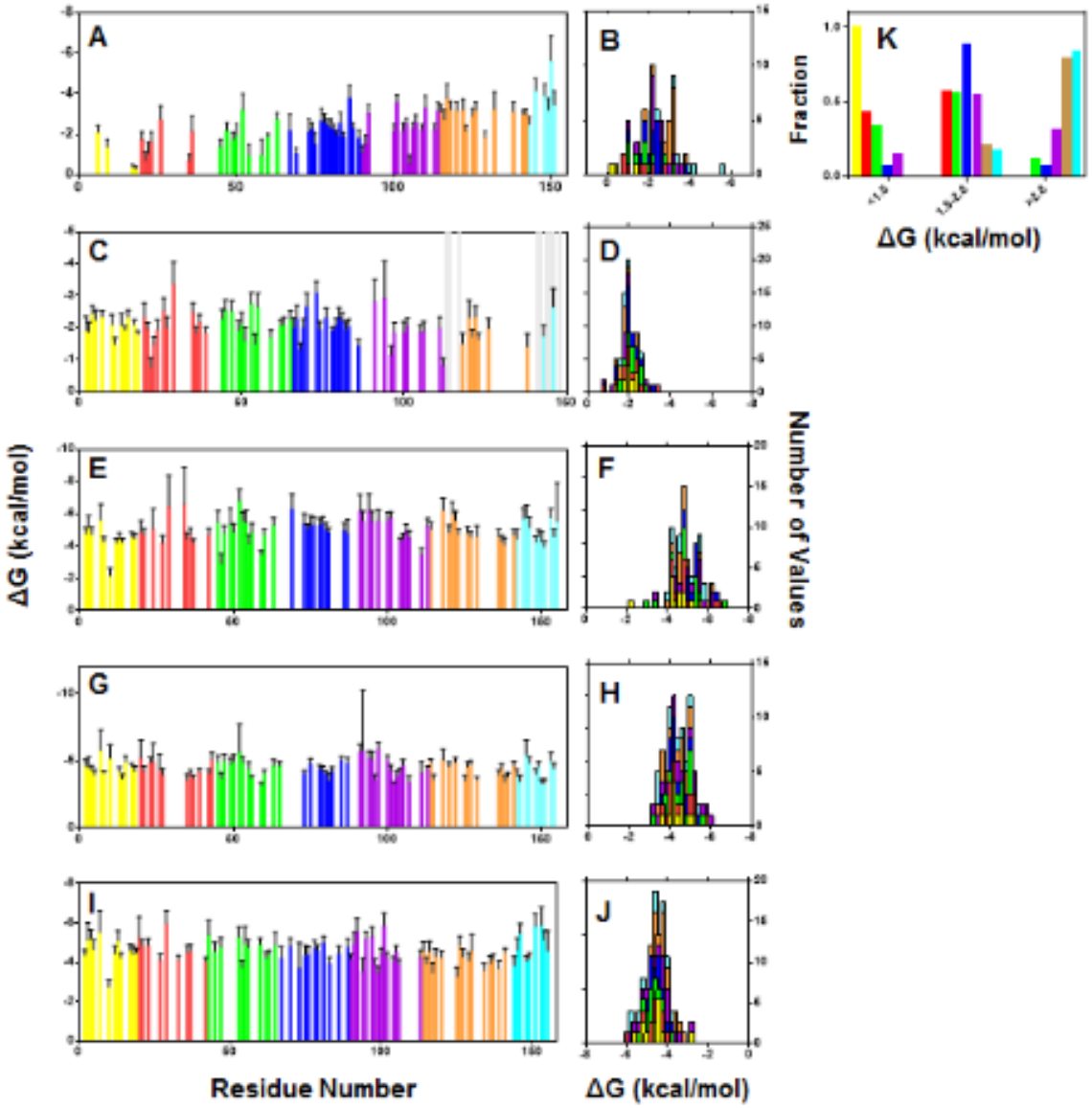

Figure S4. Repeat specific average values for the free energy changes (left column) and volume changes (right column) from analysis of the pressure-induced unfolding transitions monitored by ^{15}N-^{1}H HSQC for the pp32 cavity containing variants. (A and B) I 7A, (C and D) L60A, (E and F) L83A, (G and H) L109A and (I and J) L139A. Errors represent the standard deviation from the average of the ΔG or ΔV values for all residues in each repeat. (K) Fraction of residues within specified ΔG_o ranges (as indicated) for the I7A variant. Bars are color coded by repeat as in Figure 1.

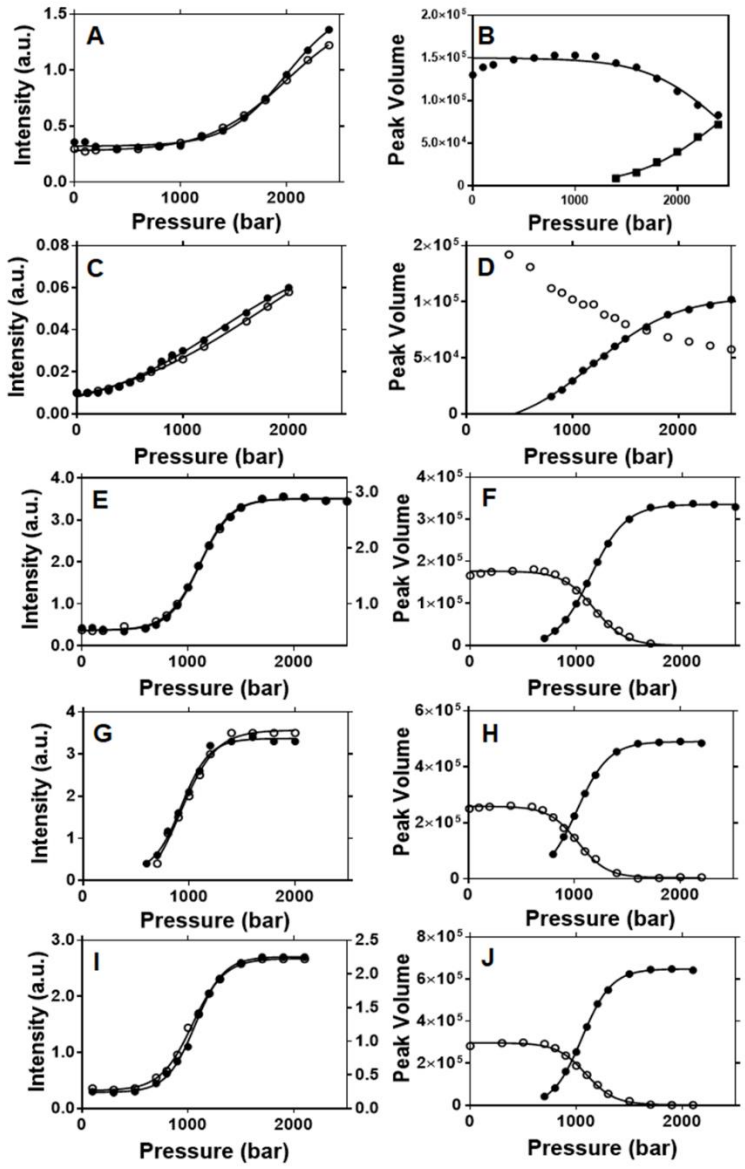

Figure S5. Pressure-induced unfolding transitions monitored by 1D-^{1}H NMR of the unfolded state sidechain methyl resonances (left column) and the Trp155 indole NH folded state (open circles) and unfolded state (closed circles) resonances for the pp32 cavity containing variants. (A and B) I 7A, (C and D) L60A, (E and F) L83A, (G and H) L109A and (I and J) L139A. Right axes in E and I correspond to the intensity values of the unfolded state methyl peak at 0.85 ppm, while left axes correspond to that at 0.92 ppm. Scales were chose such that the total changes were normalized. In A, C and G, both peaks are plotted on the same scale. The profiles from the Trp155 F and U peaks were fit globally, linking the free energy and volume changes. In B it was assumed that the plateau values for F and U were interconverted, i.e., that the value at high pressure for the F peak was zero and that for the U peak was the initial intensity of the F peak.

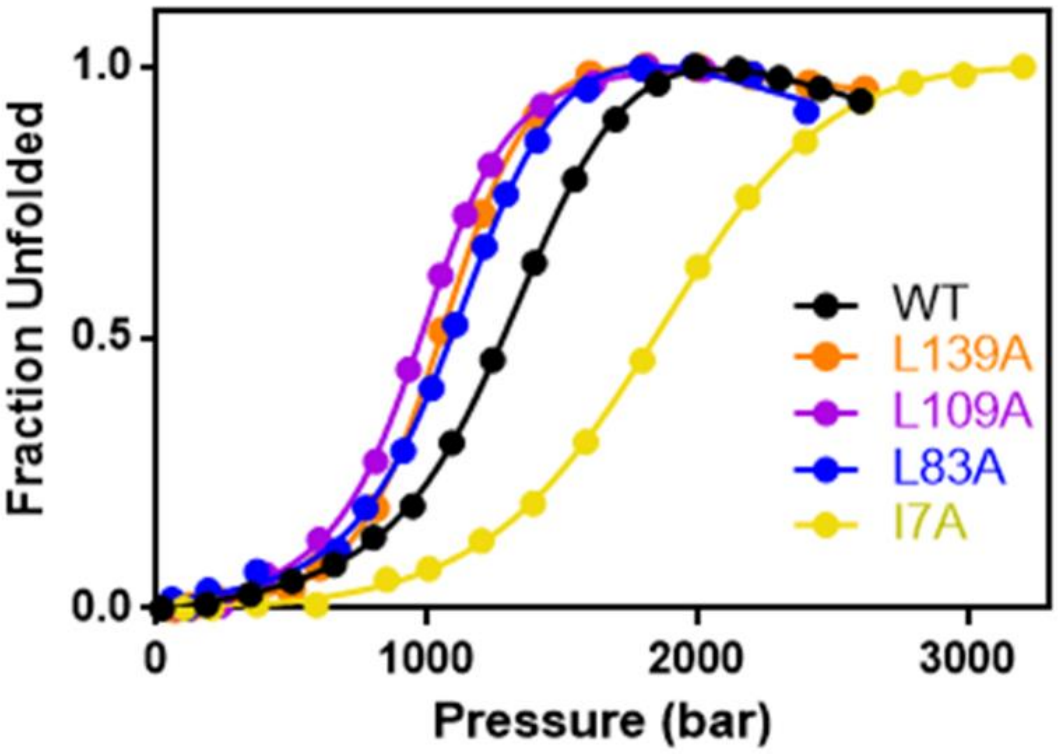

Figure S6. Fluorescence-detected pressure-induced unfolding of the pp32 variants. WT pp32 was measured in the presence of 1.4 M urea, while pp32 I7A was measured in the presence of 0.3 M urea. No urea was present in any of the other samples. Raw intensity values were fit to a two state unfolding model according to eq. 2 in the main text. Fits of WT, L83A, L109A and L139A included a high pressure baseline. Both data and fit were normalized and plotted as fraction unfolded vs. pressure.

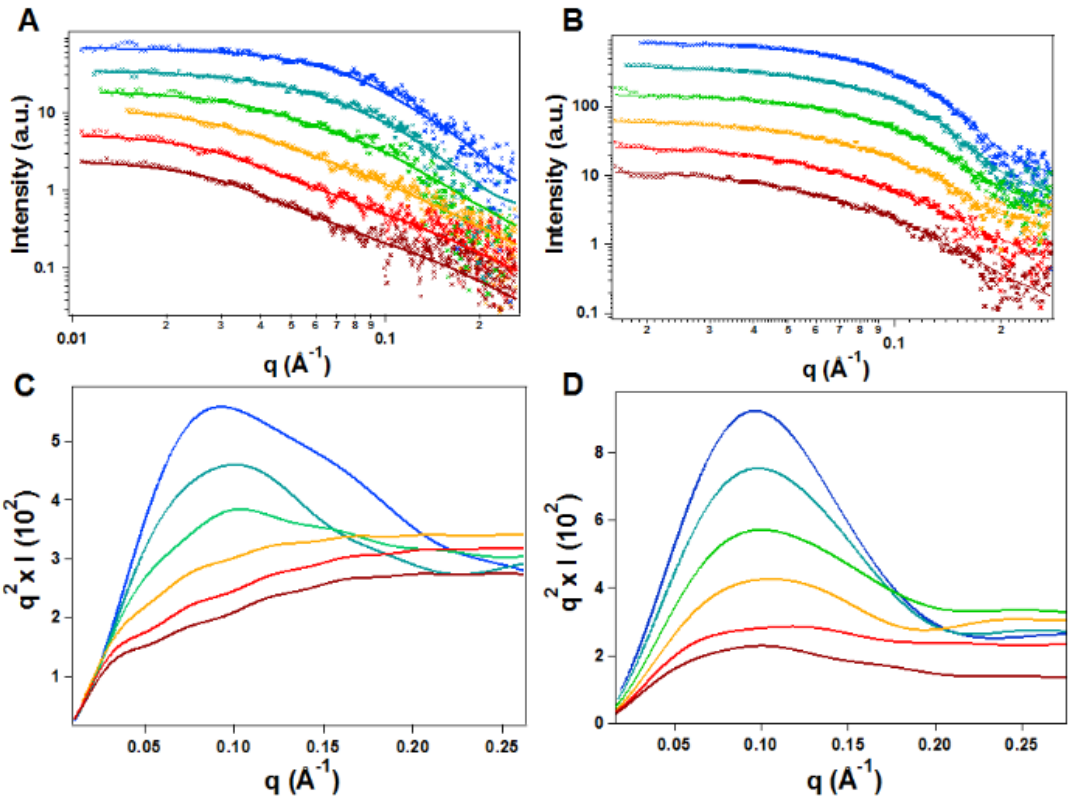

Figure S7. HP SAXS results for pp32 I7A and L139A. A and B) Scattering intensity vs. momentum transfer for pp32 L139A (A) and I7A (B (C and D) Kratky plots at increasing pressures for pp32 L139A (C) and I7A (D). For L139A (A and C), blue corresponds to atmospheric pressure, cyan to 0.4 kbar, green to 0.8 kbar, orange to 1.2 kbar, red to 1.6 kbar, and brown to 2.0 kbar. For I7A (B and D), blue corresponds to atmospheric pressure, cyan to 0.7 kbar, green to 1.4 kbar, orange to 2 kbar, pink to 2.8 kbar and red to 3.5 kbar.

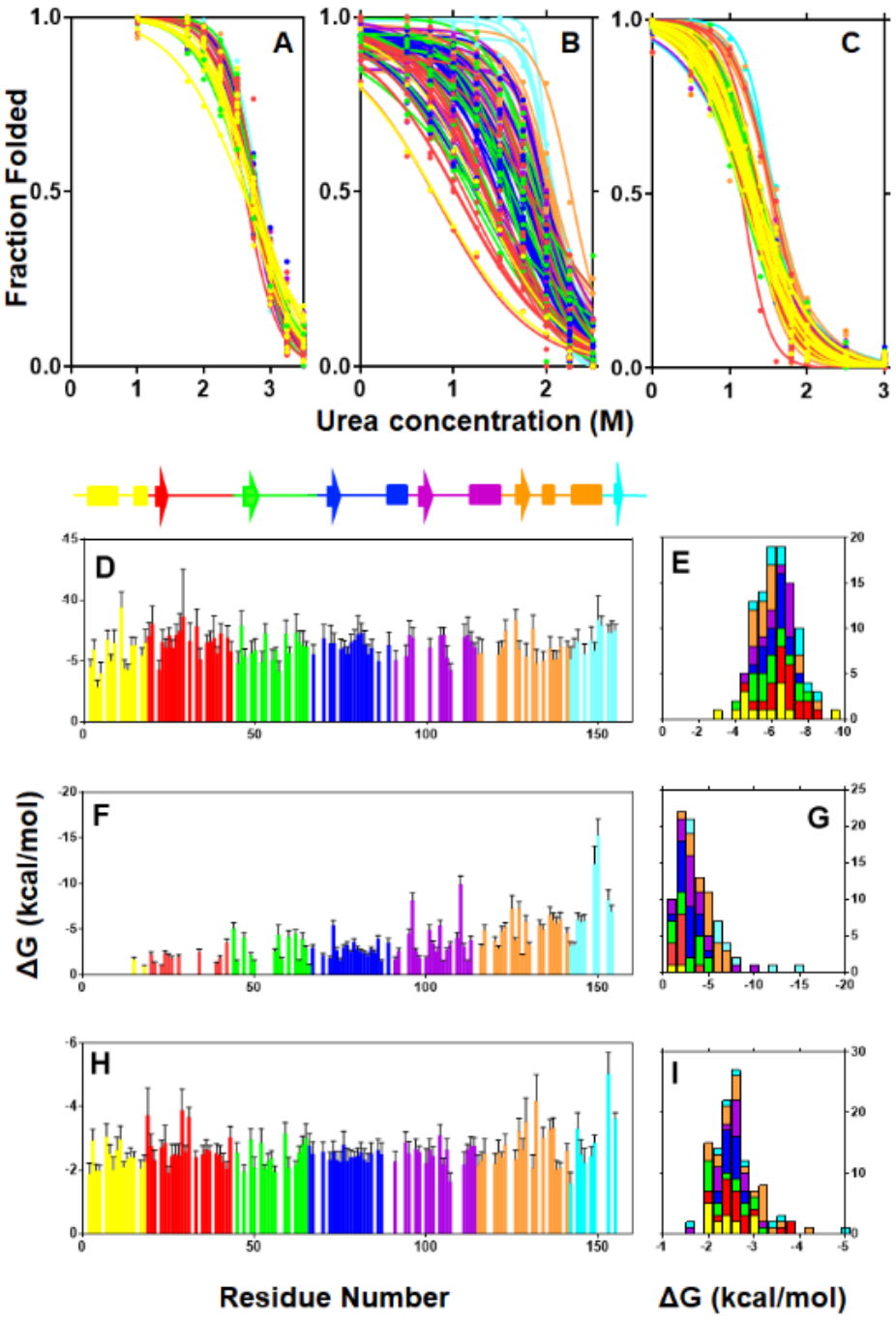

Figure S8. HSQC-detected urea induced unfolding of WT pp32 and the I7A and L60A variants. (A-C) Individual residue unfolding profiles from the amide NH resonances of (A) WT pp32, (B) I7A and (C) L60A. (D-I) Free energy changes from the profiles in A-C for (D and E) WT pp32, (F and G) I7A and (H and I) L60A. Curves and bars are colored by repeat as in Figure 1.

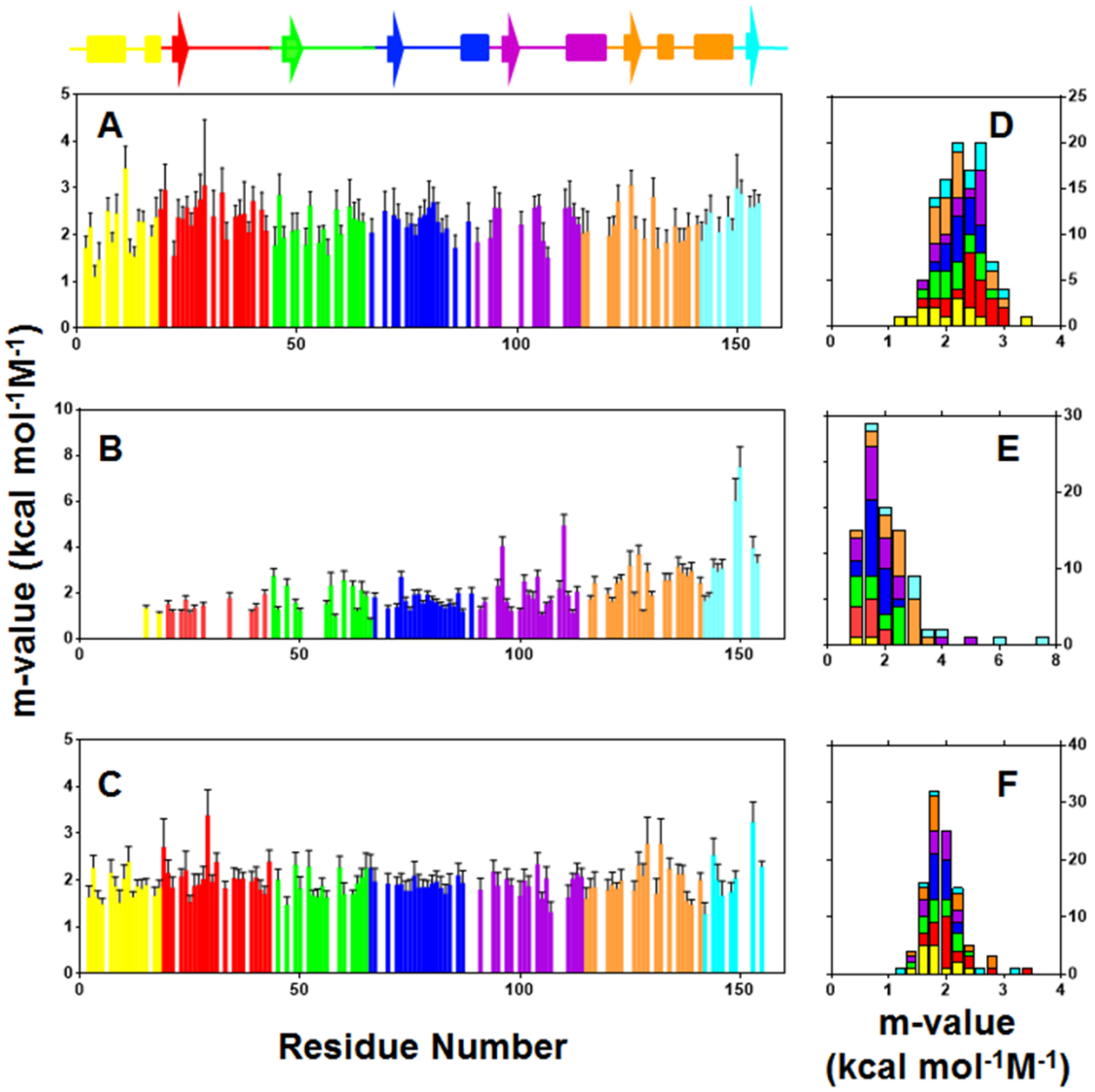

Figure S9. Residues specific m-values from the HSQC-detected urea induced unfolding of WT pp32 and the I7A and L60A variants. (A and D) WT pp32, (B and E) I7A and (C and F) L60A. Bars are colored by repeat as in Figure 1.

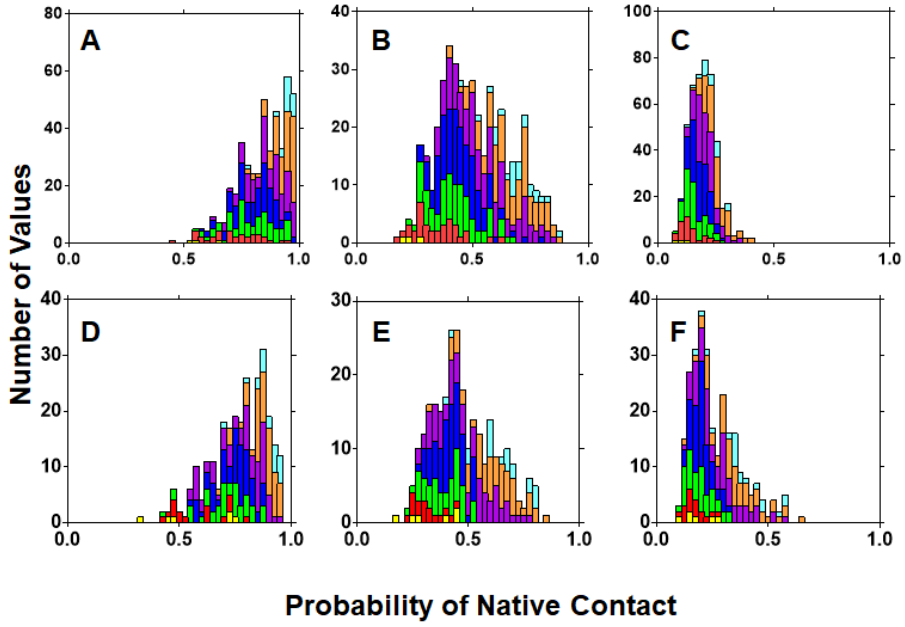

Figure S10. Contact histograms for I7A at different urea concentrations and pressures. Native contact histograms at (A) 1M urea, (B) 1.75 M urea and (C) 2.25 M urea, D) 800 bar, (E) 1600 bar and (F) 2000 bar. Fractional contacts were calculated as described in the Materials and Methods section.

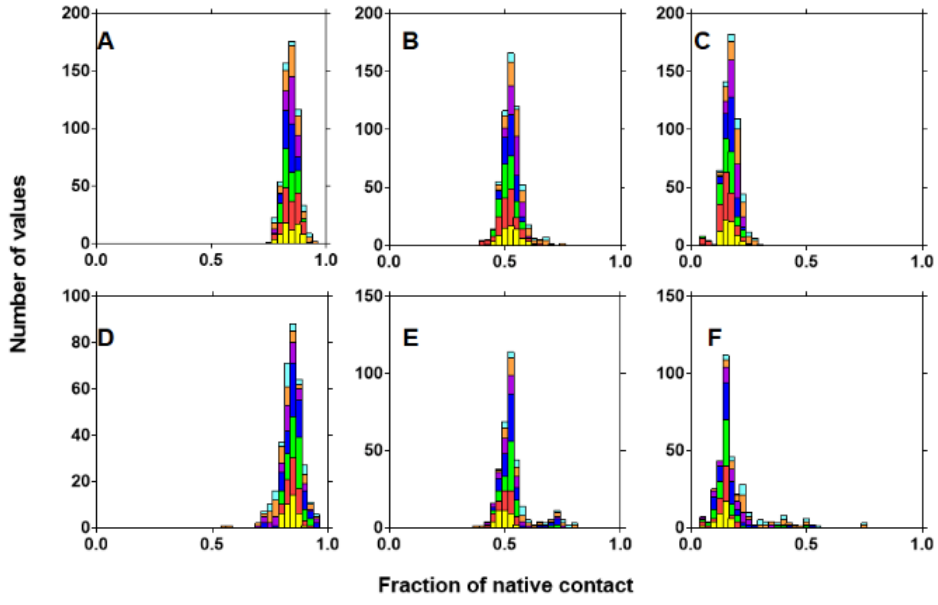

Figure S11. Contact histograms for L60A at different urea concentrations and pressures. Native contact histograms at (A) L60A at 0.75 M urea, (B) L60A 1.25 M urea, (C) 1.75 M urea, (D) 300 bar, (E) 600 bar and (F) 900 bar. Fractional contacts were calculated as described in the Materials and Methods section.